J. Mater. Environ. Sci. 6 (4) (2015) 989-996
ISSN : 2028-2508
CODEN: JMESCN

X-ray powder diffraction and Raman vibrational study of new doped compound $TiTe_3O_8$:Ce^{4+}

N. Ghribi[1*], R. Karray[1], J.P. Laval[2], A. Kabadou[1] and A. Ben Salah[1]

1 *Laboratoire des Sciences des Matériaux et d'Environnement, Faculté des Sciences de Sfax-3018, Tunisia*
2 Laboratoire des Procédés Céramiques et de Traitements de Surface, Limoges, France.

Received 24 July 2014; Revised 5 January 2015; Accepted 6 January 2015.
[*]Corresponding Author. E-mail: ghribi_nabila@yahoo.com; Tel: (+216 20 57 98 39, +033 07 62 89 95 77)

Abstract

A novel mixed tellurium oxide, $Ce_{0.07}Ti_{0.93}Te_3O_8$, has been synthesized and its crystal structure was determined from X-ray powder diffraction data. Rietveld refinement led to final confidence factors R_p=10.3% and R_{wp}=15.3%. This oxide, which crystallizes in a cubic unit-cell I $a\bar{3}$ as MTe_3O_8-type framework with cell parameter a=10.985(9) Å, exhibits a structure built up of TeO_4E (*E*= Electronic lone pair of Te(IV) disphnoids and regular Ce/TiO_6 octahedra. The crystal structure cohesion is ensured via Te–O(1)–Ce/Ti and Te–O(2)–Te bridges. The Raman spectrum is dominated by a strong band near 470 cm^{-1} and a weaker one near 650 cm^{-1} leading to a chemically symmetric Te–O(1)–Ce/Ti bridges.

Keywords: Mixed tellurium oxide; Synthesis; X-ray powder diffraction; Rietveld refinement; Tellurite; Electronic lone pairs; Raman spectroscopy.

1. Introduction

For several years, the tellurium based materials are the subject of many studies through their important properties especially in non-linear optics [1], but so far, the remarkable properties of the tellurite and tellurium dioxide in crystalline or glassy State, received no clear demonstration [2]. Such a phenomenon is clearly related to the peculiar crystallochemical behavior of Te(IV) atoms whose lone pair E is stereochemically active [3]. This activity is often reinforced, in the crystal state, when a second lone pair holder is associated with the Te(IV) atoms.

The structural polymerization of the units contributes strongly to the origin of these properties; the introduction by adding in the matrix another oxide enhances the optical properties.

Generally, this addition leads to a transformation of trigonal bipyramidal TeO_4E to TeO_3E tetrahedra with an hyperpolarizability decay. The TeO_2-based materials as MTe_3O_8 [3] tellurites; M=Ti, Hf, Sn, or Zr are known to have typical high symmetry crystal structures. It is difficult to form pure MTe_3O_8 by solid state reactions of MO_2 and TeO_2 because of the rapid TeO_2 volatilization at high temperatures.

A few investigations have been attempted on the formation of $TiTe_3O_8$ [4], this compound crystallizes in Ia-3 cubic space group, with lattice parameter: a = 10.956(3) Å. $TiTe_3O_8$ is isostructural to $SnTe_3O_8$ and $ZrTe_3O_8$ [3]. The cation forms an ordered f.c.c subcell. The titanium atom has an octahedral coordination and the tellurium atom is surrounded as in TeO_2.

In the present study, we report the preparation of a new crystalline phase, by partial substitution of the titanium atom with cerium atom. The experimental data on the structural and vibrational properties of the $Ce_{0.07}Ti_{0.93}Te_3O_8$ lattice are performed for the first time.

2. Materials and methods

The $Ce_{0.07}Ti_{0.93}Te_3O_8$ mixture compound was synthesized by using TeO_2, CeO_2 and TiO_2 (99.99%) as starting materials in a molar ratio of 3:1/2:1/2 respectively. The mixture was weighted and introduced into a silica tube which was then pumped to vacuum. The mixture was next heated during 12 hours at 600°C. The cooling rate was 1°C/min up to room temperature. Pale yellow polycrystalline powder $Ce_{0.07}Ti_{0.93}Te_3O_8$ was obtained.

The powder was mounted in the top-loaded sample holder and investigated by X-ray powder diffraction (XRPD). X-ray powder data were collected at room temperature using a SIEMENS D5000 diffractometer equipped with a monochromatic copper radiation $K_{\alpha 1}$ (λ = 1.5406 Å) with constant (2θ) steps of 0.0119. The X-ray powder diffraction data were refined by the Rietveld method [5, 6] using the FULLPROF program [7].
X-ray powder diffraction pattern reveals the coexistence of peaks relative to the α-TeO_2 paratellurite phase with those of the new prepared phase, which is no longer a problem thanks to the new version of FULLPROF [7] that make possible the multi-phase refining at the same time. It was assumed that the mixed compound is isotypic with $TiTe_3O_8$ compound [4]. Our assumption was subsequently confirmed by successful Rietveld refinement of the investigated structure.

The Rietveld refinement was carried out with the pseudo-Voigt function [8] used for the simulation of the peak shapes. In a first step, a Le Bail profile refinement was used to find the profile and instrumental parameters such as the zero error and asymmetry effects. The background was fitted with a linear interpolation between the 52 given points. The refinement with the halfwidth parameters U, V, W, unit cell parameters mixing coefficient η and the symmetry parameters converged to χ^2 = 6.89%. Then the assumed structure was refined while fixing the profile and instrumental parameters. A final refinement taking into account the overall isotropic displacement factor, converged to R_P = 10.3%, R_{wp} = 15.3% and R_{exp} = 7.18%. The occupancy probability of the Ce and Ti atoms was refined in such a way that the 8(a) site was totally occupied.

Crystal structure data and experimental conditions are collected in Table1. Positions and isotropic thermal parameters are presented in Table 2. The lattice parameters and the bond distances for both $Ce_{0.07}Ti_{0.93}Te_3O_8$ and $TiTe_3O_8$ [4] samples are reported in Table 3. Figure 1 illustrates the final Rietveld plot for $Ce_{0.07}Ti_{0.93}Te_3O_8$. The Raman spectrum was recorded in the 50-1000 cm^{-1} range using a T64000 Jobin-Yvon spectrophotometer operating in triple subtractive configuration equipped with a liquid nitrogen-cooled CCD detector. The instrument is equipped with 632.8 nm He–Ne laser.

Table 1: Experimental conditions and crystal structure data of $Ce_{0.07}Ti_{0.93}Te_3O_8$

Formula	$Ce_{0.07}Ti_{0.93}Te_3O_8$
Temperature (K)	293
Space group	$I\,a\bar{3}$
a (Å)	10.985(9)
V(Å^3)	1325.92(1)
Z	8
D_x	6.1252
Radiation (Å)	Cu K_α (1.5406)
Diffractometer	Transmission geometry (STOE)
2θ Range of refinement(°)	5-120
Number of structural variables	12
Number of profile parameters	78
R_P (%)	10.3
R_{wp} (%)	15.3
R_{exp}	7.18
χ^2 (%)	4.55
R_{bragg} (%)	4.86

Table 2: Equivalent positions and isotropic thermal parameters of $Ce_{0.07}Ti_{0.93}Te_3O_8$.

Atoms	site	x	y	z	B_{iso}(Å^2)	Multiplicity
Te	24d	0.00	0.25	0.039(8)	2.361(2)	1.00
Ti	8a	0.25	0.25	0.25	3.105(9)	0.964(2)
Ce	8a	0.25	0.25	0.25	3.105(9)	0.035(2)
O1	16c	0.919(2)	0.919(2)	0.919(2)	3.53(5)	1.00
O2	48e	0.119(1)	0.310(7)	0.149(1)	1.94(9)	1.00

Table 3: Lattice parameters and interatomic distances for $TiTe_3O_8$ and $Ce_{0.07}Ti_{0.93}Te_3O_8$ samples.

Compound	a(Å)	Te-O2 (Å)	Te-O1 (Å)	Ce/Ti-O2 (Å)
$TiTe_3O_8$	10.956(1)	1.880(3)	2.11(7)	1.953(2)
$Ce_{0.07}Ti_{0.93}Te_3O_8$	10.985(9)	1.906(4)	2.11(2)	1.925(3)

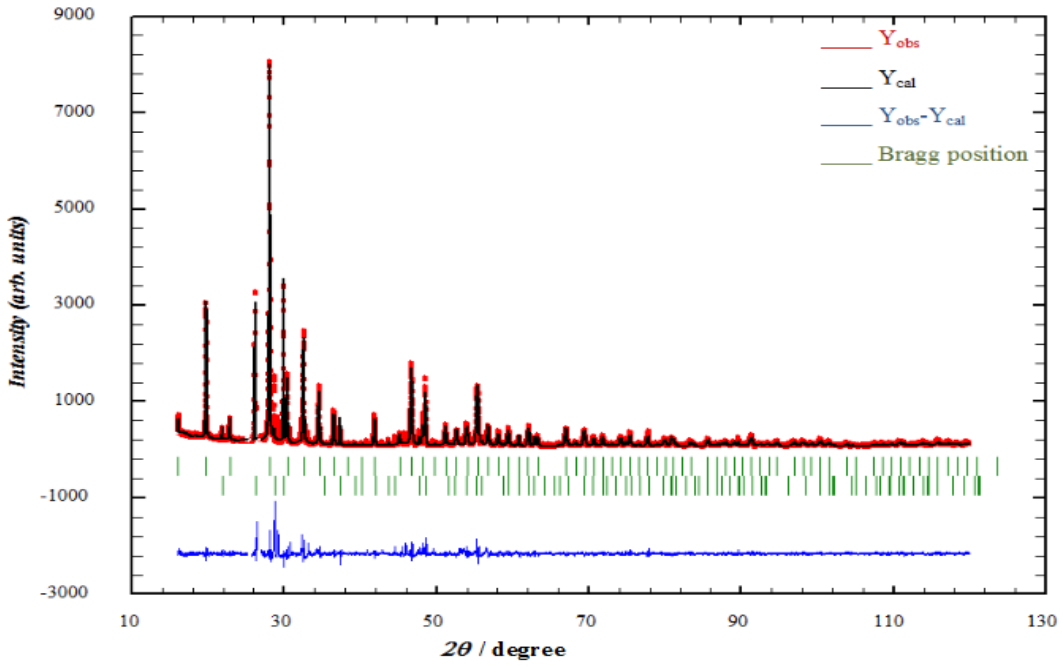

Figure 1: X-ray powder diffraction pattern and refinement of $Ce_{0.07}Ti_{0.93}Te_3O_8$.

3. Results and discussion

3.1 Bond Valence

The bond valence (S_{ij}) is given by S_{ij}= exp [(R_0- R_{ij})/B] where R_0 and B are the experimentally determined parameters and R_{ij} is the bond length of the cation – anion pair [9]. Based on the valence sum rule, the sum of the bond valence ($\sum_j S_{ij}$) around an ion must be equal to the formal valence (V_i) of this ion.

3.2 Structure determination

Structure description:

Graphical representation of the $Ce_{0.07}Ti_{0.93}Te_3O_8$ structure was performed using DIAMOND [10] (Crystal Impact and Powder Cell). The Te atoms occupy the 24*d* sites of the *Ia-3* space group, surrounded by oxygen atoms lying in the 48*e* and 16*c* positions. The Ti or Ce atoms occupy the 8*a* (0.25, 0.25, 0.25) sites.

A projection of the unit-cell content structure onto the ab plane and its perspective view are shown in Figures 2 and 3, respectively. The atomic arrangements of coordination polyhedra of cations are represented in Figure 4.

As usually observed in all tellurium oxide compounds, the distribution of the chemical bonds around the Te atoms is highly anisotropic. This asymmetry is due to the presence of the stereo-active lone pair $5s^2$. Two Te–O(2) bonds have lengths of 1.906 (4) Å and form the angle 101°,17(4), which is rather close to the atomic arrangement in the isolated TeO_2 molecule [11]. Every atom of Te has the two new neighbouring oxygen atoms of O(1) type separated from him for about 2.11(2)Å. Thus, with the four nearest oxygen atoms, each Te atom (bond valence sum of 3.82) builds a TeO_4E polyhedron in view of a trigonal bipyramid, called disphenoid. Its 'axis' is formed by the two long Te–O bonds, whereas the equatorial plane includes the two short Te–O bonds and the $5s^2$ lone electron pair *E* pointing in the direction of the third equatorial corner. These short bonds are called 'equatorial' and the long ones 'axial'.

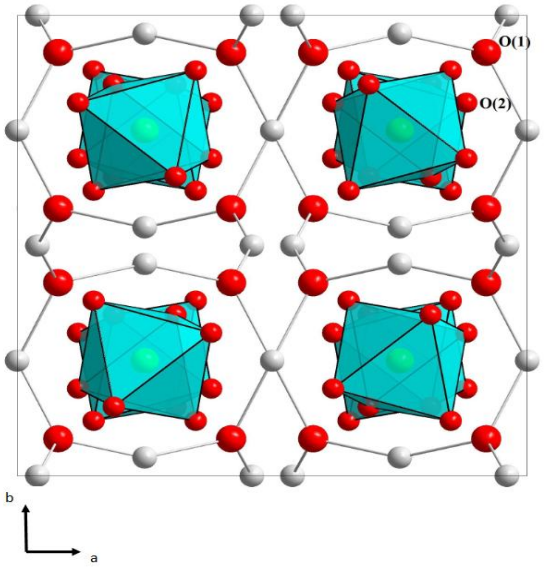

Figure 2: Projection on the ab plane of the $Ce_{0.07}Ti_{0.93}Te_3O_8$ unit cell.

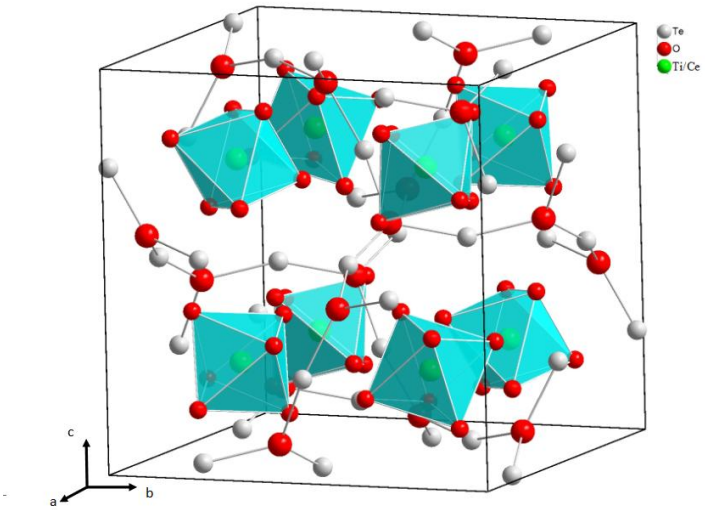

Figure 3: Perspective view of the $Ce_{0.07}Ti_{0.93}Te_3O_8$ unit cell showing the titanium/cerium polyhedron.

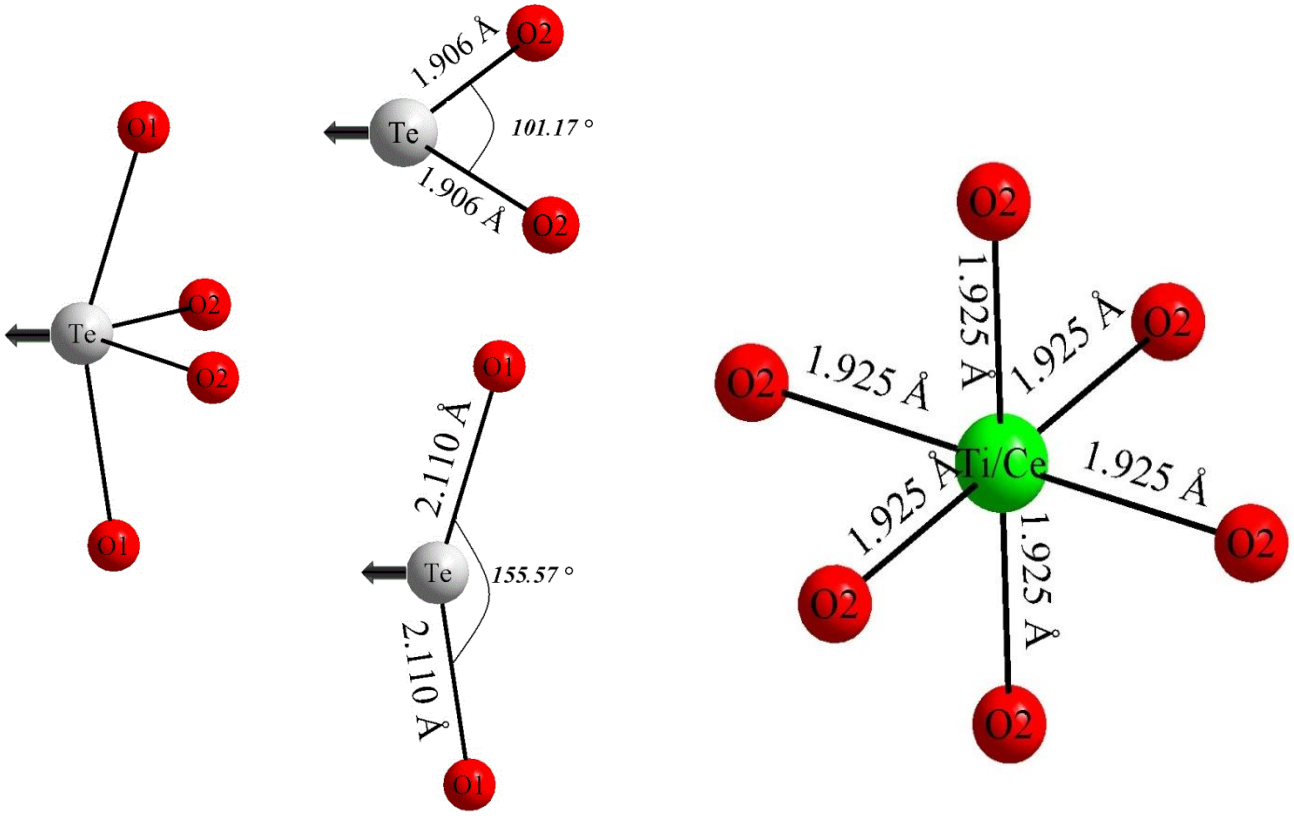

a) **b)-**

Figure 4: a)-The tellurium polyhedron in $Ce_{0.07}Ti_{0.93}Te_3O_8$.
b)-The polyhedron of cerium/titanium atoms in $Ce_{0.07}Ti_{0.93}Te_3O_8$.

The Te –O chemical bonds, are situated on one side of the Te atom, whereas the other side is a ‘dead’ zone around the lone pair E of the Te atom involving two non-bonding Te…O contacts (2.933 Å) which form ‘empty’ cavities. Due to such a sharp asymmetry of the atomic arrangement of the first coordination spheres,

the TeO_4 polyhedra have strong dipole moments which provide considerable dipole-dipole contribution to the inter-anion potentials.

TeO_4 neighbouring disphenoids are interconnected via a common corner without having common O–O edges (Figure 5).

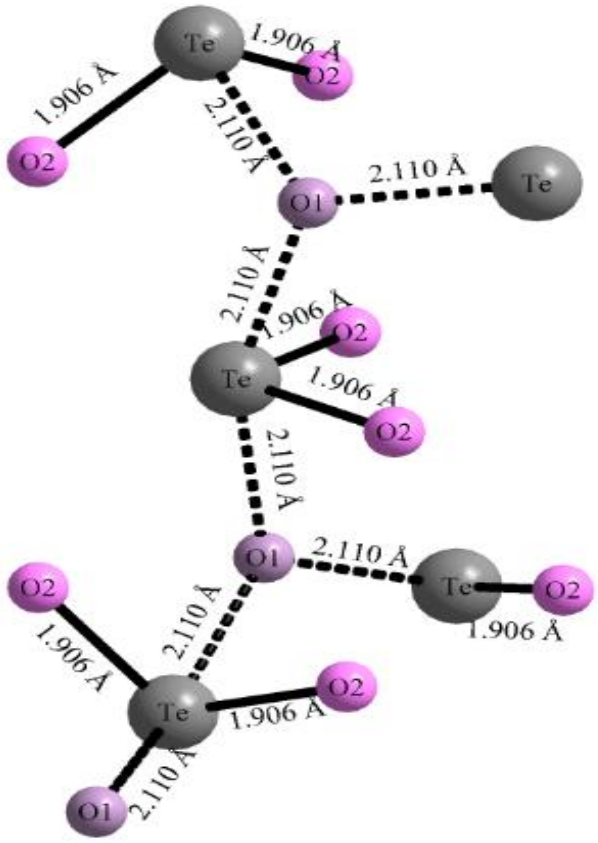

Figure 5: Interconnecting neighbouring tellurium disphenoids.

The Ce/Ti atoms are sixfold coordinated with O(1)-type oxygen atoms forming a slightly distorted octahedron with Ce/Ti-O distances of about 1.92(3) Å (bond valence sum of 4.46) and O-Ce/Ti-O angles varying from 88.28(1)° to 179.99(4)°.

Oxygen atoms occupy two different positions, forming the Te–O(1)–Ce/Ti and Te–O(2)–Te bridges, thus ensuring crystal structure cohesion.

This structural study showed $Ce_{0.07}Ti_{0.93}Te_3O_8$ crystalline phase to have a structure almost identical to that of $TiTe_3O_8$ compound. This result is not surprising, since the chemical composition of the sample studied here, approaches closely that of $TiTe_3O_8$ compound.

The Ce/Ti–O2 bond distance (1.92(3) Å) is slightly shorter than that observed for $TiTe_3O_8$ (1.95 (3) Å),

The Te–O1 bond distance (2.11(2) Å) is identical to the value observed for $TiTe_3O_8$, while the Te–O2 bond length (1.90(4) Å) is slightly larger (1.88 Å) inducing lattice parameter increasing from 10.956 to 10.985 Å.

This feature is probably due to the slight differences in chemical composition between the two samples. A Raman study was carried out to confirm these results.

Vibrational study:

The Raman study was limited to the frequency range 50 to 1000 cm^{-1}. The Raman scattering of the synthesized phase is given in Figure 6, in addition to crystalline α-TeO_2 and $TiTe_3O_8$ phase's spectra.

It is useful to recall some general features inherent for the Raman spectra of such oxides lattices. If atom X is much harder than oxygen, the middle-frequency and the highest-frequency parts of the spectra are associated with the displacements of the oxygen atoms, and can be described in terms of localized stretching vibrations of the X–O–X bridges.

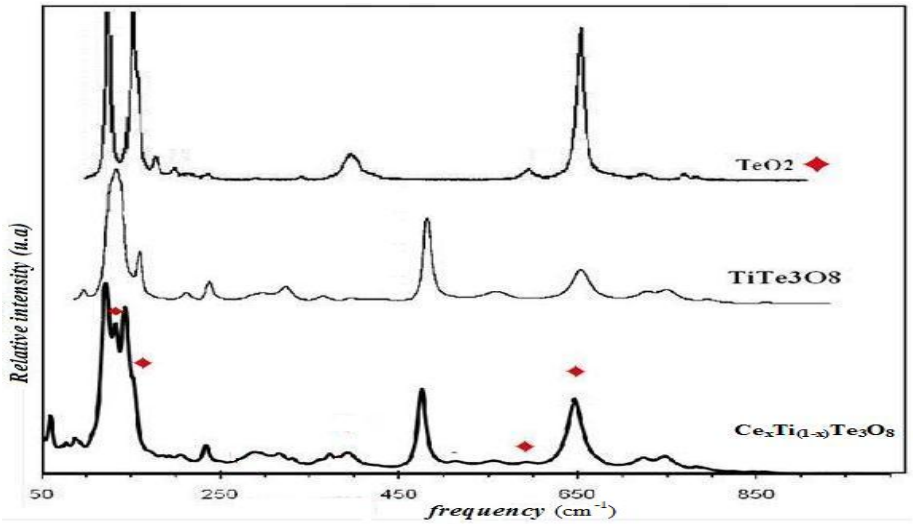

Figure 6: Raman spectra of $Ce_{0.07}Ti_{0.93}Te_3O_{8,}$ α-TeO_2 and $TiTe_3O_8$ crystalline phases.

The Raman intensity of the asymmetric X–O–X stretching vibrations (occupying the highest frequency range) is related to the difference in the electronic polarizability properties of the two bonds involved on the X–O–X bridge. Consequently, if the bonds are identical, those vibrations would have a vanishing intensity in the Raman spectra. Contrary to this, the symmetric X–O–X stretching vibrations lying in the middle-frequency part of the spectrum would produce the strongest lines [1, 12] (Figure 7).

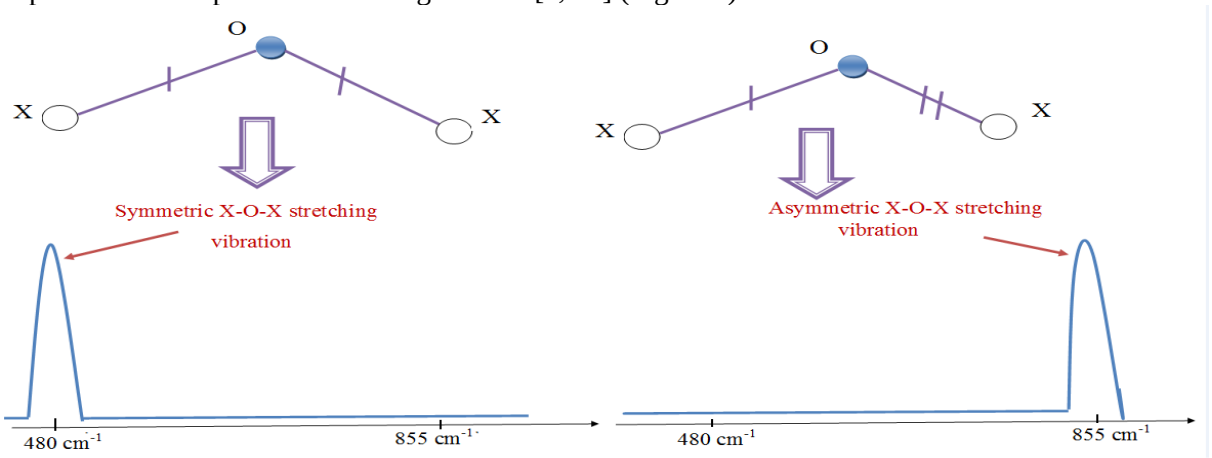

Figure 7: The shape of Raman spectra in both compounds characterised with symmetric and asymmetric X-O-X bridges.

It can be added that intense Raman-active bands in the region of the high-frequency stretching vibrations of oxide lattices would be necessarily related to the non-bridging (terminal) X–O bonds [13]. So, if the Raman spectrum of any oxide structure contains the intense bands in the highest frequency range, but such bands are absent in the middle–frequency range, it can be thought that this structure does not possess the X–O–X bridges.

Consequently, if a given Raman spectrum has the strong bands in the middle-frequency range and in the high-frequency range simultaneously, both terminal X–O bonds and X–O–X bridges would be present in the relevant structure, as the independent structural fragments.

Thus, the intensities of bands in Raman spectra offer a capability for clarifying the valence electron distribution patterns (i.e., the character of an interatomic bonding) in condensed oxides.

The energetic criterion for the formation of the tellurite anions, i.e., for the augmentation of the number of the Te–O bonds, comes from the difference between the energies of these bonds and the M–O bonds in the modifier. Evidently, the weaker the M–O bonds are, i.e., the weaker the M cation, the more vigorously the modifier acts on TeO_2, i.e. the stronger it is. Indeed, if the modifier transfers all of its oxygen ions to the tellurium, it can be considered as a ‘strong’ modifier.

The existence of the paratellurite α-TeO_2 is confirmed by examining the experimental spectrum where the indicate peaks were attributed to this phase. Indeed, the Raman spectrum of the α-TeO_2 lattice shows the presence of two intense peaks (123 and 175cm^{-1}) corresponding to translation and rotation movement of isolated TeO_2 entities, respectively, the weak band near 592 cm^{-1} is attributed to antisymmetric stretching vibrations. It is dominated by the strong high–frequency stretching vibrations (650 cm^{-1}), and has rather weak lines in the middle-frequency part (390 cm^{-1}). Thus, the presence of the largely covalent terminal Te–O bond is clearly manifested there, whereas none of the lines in this spectrum indicates the existence of Te–O–Te bridges made of such bonds. Therefore, from the objective spectrochemical point of view, the α-TeO_2 lattice is not considered as a classic framework, but rather as island-type one, i.e. this built up from the quasi 'isolated' TeO_2 molecules whose synchronous pulsation is account for the high frequency strongest bands.

Within the framework of this conception Ce_{IV} and Ti_{IV} are considered as falling in the category of cations whose field strengths are intermediate [14].

Concerning the new phase $Ce_{0.07}Ti_{0.93}Te_3O_8$, the Raman spectrum is characterized by an intense band at about 475 cm^{-1}. Above this band we observe height of lower intensity as that at 650 cm^{-1} which is relatively intense and that at 859 cm^{-1} which is very weak. The peak observed around 385 cm^{-1} is similar to that of the $CeTe_2O_6$ crystalline phase [15] and is attributed to the symmetric vibration of the Te-O-Ce bridges. No stretching bonds relative to $(TeO_3)^{2-}$ *ortho*-anions are observed.

It must be particularly underlined that the absence of strong bands in the high-frequency (stretching) region of the spectrum shows that this structure is a framework in which neither Ce/Ti–O bonds, nor Te–O bonds can be considered as terminal ones, but forming the covalently bonded Te–O–Ce/Ti bridges. The intense band observed at 480 cm^{-1} is assigned to symmetric stretching vibration of Te-O- Ce/Ti bridges. While that observed at 859cm^{-1} is attributed to the asymmetric stretching. The assignment of these two bands is the same whatever the considered cation (Ti, Zr and Sn) [16, 17], whereas theirs intensities vary with the cation nature. Therefore the Raman scatterings of $TiTe_3O_8$, $SnTe_3O_8$, $ZrTe_3O_8$ and $Ce_{0.07}Ti_{0.93}Te_3O_8$ are given in the Figure 8 for comparison.

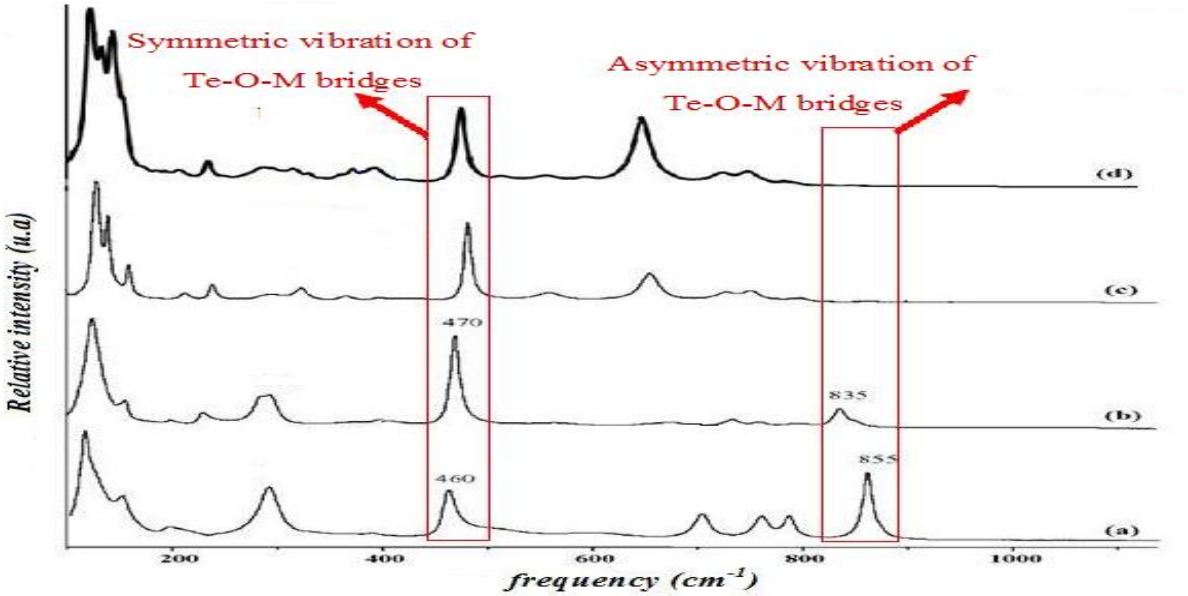

Figure 8: (a) Raman Spectrum of crystalline phase $ZrTe_3O_8$.
(b) Raman Spectrum of crystalline phase $SnTe_3O_8$.
(c) Raman Spectrum of crystalline phase $TiTe_3O_8$.
(d) Raman Spectrum of crystalline phase $Ce_{0.07}Ti_{0.93}Te_3O_8$.

In the $ZrTe_3O_8$ compound structure the Te-O (2) bond length is 1.858 Å and that of Zr-O(2) is 2.073 Å, as these values are quite different and consequently the links are not chemically equivalent, this follow-on in the Raman spectrum by the presence of an intense band around 855 cm^{-1} characteristic of Te-O-Zr bridges asymmetric stretching vibration.

While in the $SnTe_3O_8$ compound structure, the difference between Te-O (2) and Sn-O(2) length becomes less important that is to say the linkages are more chemically equivalent (Te-O (2) length is 1.867 Å and that of Sn-O (2) is 2.05 Å) giving more symmetric Te-O(2)-Sn bridges, therefore on the Raman spectrum, the band intensity at 835 cm^{-1} decreased while and that of the band around 470 cm^{-1} increased, indicating that the Te-O(2)-Sn bridges are more symmetrical than Te-O (2)-Zr ones.
In the case of the $TiTe_3O_8$ crystalline phase, the Te-O(2) and Ti-O(2) lengths are very nearly, respectively 1,883 and 1,953 Å. As a result, symmetric stretching vibrations of Te-O-Ti bridges give rise to an intense band situated near 480 cm^{-1} whereas the asymmetric stretching have very weak intensities and are localized at about 859 cm^{-1}. According to these observations and since the Raman scattering spectrum of $Ce_{0.07}Ti_{0.93}Te_3O_8$ crystalline phase is characterized by a very intense band at 470 cm^{-1}, whereas the band at 850 cm^{-1} vanished, we can deduce that the Te-O and Ce/Ti-O bonds are chemically equivalent and then the Te–O(1)–Ce/Ti bridges are chemically symmetric.

Conclusion

In the new synthesized $Ce_{0.07}Ti_{0.93}Te_3O_8$ structure, Ce/TiO_6 octahedrons and the TeO_2 quasi-molecular units compose a three-dimensional framework in which oxygen atoms occupy two different positions, thus forming the Te–O–Ce/Ti and Te–O–Te bridges. So no oxygen ions can be transferred to TeO_2, and then no tellurite anions is created. For that, from the chemical point of view, $Ce_{0.07}Ti_{0.93}Te_3O_8$ structure cannot be considered as a tellurite one, but it can be specified as "*solid solution"* of CeO_2 and TiO_2 in TeO_2.

Spectroscopically the Raman spectrum is dominated by a relatively strong band near 470 cm^{-1} and a weaker band near 650 cm^{-1}, whereas no band was detected near 850 cm^{-1} which allows us to conclude that the Te-O and Ce/Ti-O bonds are chemically equivalent and then the Te–O(1)–Ce/Ti bridges are chemically symmetric.

Acknowledgements-Authors like to thank Materials and Environmental Sciences laboratory who provided the financial support for this research project.

References

1. Yakine I., Chagraoui A., Moussaoui A., Tairi A., *J. Mater. Environ. Sci. 3 (4) (2012) 776-78.*
2. Blanchandin S., Champarnaud-Mesjard J. C., Thomas P., Frit B., *Solid State Sciences 2,* (2000) 223.
3. Yamaguchi, O., Ohtagaki T., Shimizu K., Z. *Anorg. Allg. Chem.* 564, (1988) 115.
4. Meunier G., Galy J. *Acta Crystallographica, Section B*: *Structural Crystallography and Crystal Chemistry*. 27 (1971) 602.
5. Rietveld H.M. *J. Appl. Cryst.* 2 (1969); 65.
6. Taoufyq A., Chokouadeu D.V., Bakiz B., Ait Ahsaine H., Patout L., Benlhachemi A., Ezahri M., Guinneton F., Lyoussi A., Nolibe G., Gavarri J-R, *J. Mater. Environ. Sci. 5 (S2) (2014) 2550-2554.*
7. Rodriguez-Caravajal J., Roisnel T., *Commission on Powder Diffrac, Inter. Union of Crystallo, Newsletter* (1998) 20.
8. Caglioti G., Paoletti A. Ricci F.P. *Nucl. Instrum. Methods*, 3 (1958) 201.
9. Shannon R.D, *Acta. Crystallogr. Sect* A 32 (1976) 767.
10. Diamond W. Kraus, Nolze J., *Powder. Diffrac.*13 (1998) 256.
11. Muenow D.V., Hastie J.W., Bautista R., Macgrave J.L., *Trans. Faraday Soc*., 65 (1969) 3210.
12. Mirgorodsky A.P., Merle-Mejean T., Champarnaud J.-C., Thomas P., B. Frit. *J. Phys. Chem. Solids,* 61 (2000) 501
13. Kingma K.J., Hemley R.J., *Am. Mineralog.* 79 (1994) 269.
14. McLaughlin J.-C., Tagg S.L., Zwanziger J.W., *J. Phys. Chem. B* 105 (2001) 67.
15. Meier S.F., Weber F.A., Gläser R.J., Schleid T.. *Zeitschrift für anorganische und allgemeine Chemie*, 627 (2001) 2448.
16. Sekiya T., N. Mochida, Soejima A.. *J. Non-Crystal Solids*. 191(1,2) (1995) 115.
17. Sabadel J.C., Armand P., Cachau-Herreillat D., Baldeck P., Doclot O., Ibanez A., Philippot E.. *J. Solid State Chem.* 132 (2) (1997) 411.